Journal of Inflammation Research

Dovepress
Taylor & Francis Group

Open Access Full Text Article

ORIGINAL RESEARCH

Electroacupuncture Inhibits the Early Neuroinflammatory Cascade Triggered by TLR2 in the Prodromal Period of PD

Ke Xu[1], Yuan Li[2], Bing-Cheng Hu[3], Yu Zhang[1], Yan Bai[4], Shun Wang[1]

[1]Second Clinical Medical College, Heilongjiang University of Chinese Medicine, Harbin, Heilongjiang, 150006, People's Republic of China; [2]Acupuncture Department, The First Affiliated Hospital of Harbin Medical University, Harbin, Heilongjiang, 150001, People's Republic of China; [3]Acupuncture Department Three, Heilongjiang Academy of Chinese Medicine Sciences, Harbin, Heilongjiang, 150036, People's Republic of China; [4]Acupuncture Research Institute, Heilongjiang Academy of Chinese Medicine Sciences, Harbin, Heilongjiang, 150036, People's Republic of China

Correspondence: Shun Wang; Yan Bai, Email hljwang@aliyun.com; 1447003128@qq.com

Objective: To explore electroacupuncture (EA)'s effect and mechanism in alleviating prodromal Parkinson's disease (pPD) by targeting TLR2-mediated neuroinflammation.

Methods: Rat pPD models were established via striatal 10 μg/4 μL 6-OHDA injection. EA was applied at DU20, EX-HN3, LR2, and LR3 for 14 days. Behavioral tests, ELISA, immunohistochemistry, immunofluorescence, Western blot and qRT-PCR were used to assess non-motor symptoms, DA/TH levels, TLR2 expression, microglial activation, TLR2/NF-κB/NLRP3 pathway and pyroptosis.

Results: 6-OHDA induced 30–40% striatal DA reduction and typical pPD non-motor symptoms. EA significantly improved these symptoms, reduced TLR2 expression in key regions (substantia nigra, hippocampus, etc), inhibited M1 microglial activation (decreased CD86, increased CD206), and suppressed TLR2/NF-κB/NLRP3 pathway-related proteins, and inhibits microglial pyroptosis.

Conclusion: EA inhibited the neuroinflammation and microglial cell activation as well as pyroptosis mediated by TLR2, thereby alleviating the non-motor symptoms of PD. This provides a potential possibility for the intervention treatment of PD to prevent the progression of the disease.

Keywords: electroacupuncture (EA), prodromal period of Parkinson's disease (pPD), TLR2/NF-κB/NLRP3, neuroinflammation, microglia, pyroptosis

Introduction

The prodromal period of Parkinson's disease (pPD) refers to the period marked by early symptoms or signs of neurodegenerative changes, predominantly involving non-motor symptoms such as rapid eye movement sleep behavior disorder, olfactory dysfunction, anxiety and depression, constipation, and cognitive impairment, without tremors or other motor symptoms.[1] Dopaminergic neurons located in the substantia nigra regulate the nigrostriatal pathway, through which dopamine (DA) is transported to the striatum, playing a crucial role in motor regulation within the basal ganglia circuitry.[2] The degeneration of the nigrostriatal pathway and the consequent reduction in DA neurotransmitter levels within the striatum are primarily responsible for the non-motor symptoms observed in pPD. Investigating pPD can aid in identifying early warning signs and enhancing the early detection of Parkinson's disease (PD) risk factors, thereby potentially preventing or delaying the onset of motor symptoms. In 2005, Ruediger Hilker's research team conducted a longitudinal positron emission tomography (PET) study using fluorodopa F18 and found that the onset of pPD symptoms typically occurs when DA depletion in the striatum reaches approximately 31%.[3]

Currently, several hypotheses exist concerning the pathogenesis of PD, with neuroinflammation being recognized as a key pathological mechanism. Accumulating evidence suggests that the onset of PD is closely associated with neuroinflammatory processes. Their findings demonstrate distinct neuroinflammatory features in a mouse model of PD characterized by α-synuclein (α-Syn) overexpression. Furthermore, early-stage inflammatory responses may play a critical role in the progressive deterioration

https://doi.org/10.2147/JIR.S585729
Received: 9 December 2025
Accepted: 26 February 2026
Published: 5 March 2026

of the nigrostriatal pathway.[4] The Karlijn team conducted postmortem analyses of the brains of deceased patients. This study was the first to confirm in human brain tissue that TLR2 plays a crucial role in the neuroinflammatory response during the progression of PD. Patients included in the study who were classified at Braak stages 1–3 did not exhibit clinical symptoms of PD but showed the presence of α-Syn deposits upon autopsy. Therefore, this phase is regarded as pPD. The study revealed that TLR2 expression in the substantia nigra progressively increased during the pPD (Braak stages 1–3), but declined during the clinical phase (Braak stages 4–6). Furthermore, the study demonstrated that TLR2 is significantly involved in mediating neuroinflammation during pPD progression. Given that other subtypes of the Toll-like receptor family did not exhibit comparable patterns, TLR2 is considered to be a highly specific mediator in this context.[5] As a member of the Toll-like receptor family, TLR2 can activate specific protein kinases, thereby triggering the downstream NF-κB signaling pathway and ultimately promoting the production of pro-inflammatory cytokines.[6] These findings collectively underscore TLR2 as a critical regulator of neuroinflammation in PD. However, the precise mechanisms by which TLR2 mediates neuroinflammatory processes during the pPD remain to be fully elucidated.

Electroacupuncture (EA) is a unique therapeutic approach in traditional Chinese medicine, Its primary advantages include the synergistic effects of combined therapies, a shortened treatment duration, and a reduction in adverse effects. A substantial body of research has demonstrated that EA can exert antioxidant stress responses,[7] anti-neuroinflammatory responses,[8] upregulate neurotrophic factors,[9] downregulate endoplasmic reticulum stress,[10] improve mitochondrial function,[11] activate autophagy,[12] regulate the intestinal microbiota[13] in PD, andeffectively alleviate both motor and non-motor symptoms of PD, as well as improve underlying neurodegenerative processes.[14–16]

Methods

Animals

Male Sprague-Dawley rats of clean grade (weighing 200–220g) were maintained under controlled environmental conditions, including a room temperature of 23 ± 2°C, relative humidity of 50%–70%, and a natural light-dark cycle. The animals were allowed ad libitum access to food and water, and their bedding was refreshed every three days. Prior to the commencement of the experiment, the rats were acclimatized for one week. All experimental procedures involving animals were conducted in accordance with the principles outlined in the International Animal Protection Guidelines. The study was approved by the Ethics Committee of Heilongjiang University of Traditional Chinese Medicine (Approval No. 2023122908).

6-OHDA-Induced Rat Model of the Prodromal Period of PD

The Ctrl group did not receive any treatment. In the other groups, different doses of 6-OHDA (10 μg/4 μL, 13 μg/4 μL, and 16 μg/4 μL) were administered into the left striatum at a single target site using a stereotactic apparatus, based on the corresponding stereotactic coordinates in the Paxinos and Watson brain atlas: anterior-posterior (AP) +1 mm, medio-lateral (ML) +3 mm, and dorsal-ventral (DV) -5 mm. In the Sham group, a 0.1% ascorbic acid solution was injected into the left striatum at a rate of 0.5 μL/min, with a total volume of 4 μL. In the model group, a 6-OHDA solution of 10 μg/4 μL was injected into the left striatum at the same infusion rate. The injection needle was maintained in place for 5 minutes before being slowly withdrawn. The model was evaluated 14 days post-surgery.

EA Treatment

Based on the model group, the acupoints Baihui (DU20), Yintang (EX-HN3), Xingjian (LR2), and Taichong (LR3) were selected. Baihui was paired with Yintang, while Xingjian and Taichong were selected as well, and all were connected to the G-6805 electroacupuncture apparatus. A continuous wave was applied at an intensity of approximately 1 mA, which was considered appropriate when a slight tremor of the needle handle was observed and the animal remained calm without signs of distress or vocalization. The frequency used for scalp acupuncture was set at 100 Hz, whereas limb acupuncture was performed at a frequency of 30 Hz. The needles were retained for a duration of 30 minutes, and the treatment was administered once daily for 14 consecutive days.

Enzyme-Linked Immunosorben Assay (ELISA)

The left and right striatum, substantia nigra, hippocampus, olfactory bulb, and colon tissues were carefully dissected from rats on ice and immediately stored at -80°C. The collected tissues were mechanically homogenized in physiological saline using an ice water bath at 2500 rpm for 10 minutes. Subsequently, DA and TLR2 levels were quantified using a Rat DA ELISA Kit (E-30236, Guangdong Andy Gene Biotechnology Co., Ltd) and a Rat TLR2 ELISA Kit (E-30934, Guangdong Andy Gene Biotechnology Co., Ltd), respectively, according to the manufacturer's instructions.

Immunohistochemistry (ICH)

Paraffin sections were subjected to antigen retrieval by heating in antigen retrieval solution for 10 minutes. Subsequently, the sections were immersed in PBS solution for 5 minutes, and this procedure was repeated three times. Following PBS treatment, the sections were blotted dry with absorbent paper, followed by incubation in 3% hydrogen peroxide (H_2O_2) for 15 minutes to block endogenous peroxidase activity. Thereafter, the sections were blocked with goat serum (#AR1009, Solarbio Science & Technology Co., Ltd., Beijing) to reduce nonspecific binding. After blocking, the primary antibody TH (#bs-0061r, Beijing Bioss Biotechnology Co., Ltd., dilution ratio 1:300) was applied, and the sections were incubated overnight at 4°C. Following three washes with PBS, the secondary antibody (1:400) was added, and the sections were incubated at 37°C for 45 minutes. Immunostaining was then developed using DAB substrate (#DA1016, Solarbio), followed by counterstaining with hematoxylin (#H8070, Solarbio). Finally, the sections were mounted and examined under a light microscope.

Weight Gain Rate of Rats

The body weight of rats in each group was measured in the early morning prior to feeding, and the body weight change rate was subsequently calculated. The formula for calculating the body weight change rate was as follows= (body weight after modeling – initial body weight) / initial body weight × 100%.

Preference Rate for Sucrose Solution

A two-day adaptation period will be given before the test. Each rat was allowed to freely choose to drink from a bottle of sugar water and a bottle of sterilized water within one hour. The positions of the two bottles were randomly adjusted. The sucrose solution preference rate was calculated as: [sugar water intake (g) / [sugar water intake (g) + sterilized water intake (g)]] * 100%.

Tail Suspension Stationary Time

The tails of rats were fixed to a suspension device 1 meter above the ground, causing them to hang upside down. After allowing the rats 2 minutes to adapt, the time they spent in a "static" state (defined as no obvious movement for more than 3 consecutive seconds) was recorded over the following 6 minutes.

Sleep Evaluation

The rats were intraperitoneally administered with pentobarbital sodium at a dosage of 50 mg/kg, and their sleep status was monitored. Following administration, the animals were placed on a flat surface in a supine position with their abdominal side facing upward. A sustained supine posture without movement for more than 60 seconds was considered as the loss of the righting reflex, indicating the onset of sleep. During the sleep phase, two or more body turns within a 60-second interval were interpreted as the return of the righting reflex, suggesting the animal had regained consciousness. Sleep latency, defined as the time interval from drug administration to the absence of the righting reflex, and sleep duration, defined as the period from the loss of the righting reflex to the resumption of spontaneous activity, were recorded.

Burial Feeding Experiment

Three days prior to the commencement of the test, food intake for the rats was restricted. During the regular feeding period, food lumps (cornflakes coated with honey) were introduced while ensuring an adequate and continuous supply of water. At the beginning of the experiment, each rat cage was provided with a clean bedding layer of sufficient quantity and uniform thickness, at least 3 cm deep. A food lump of standardized size was randomly buried 1 cm beneath the surface of the bedding in

each cage. Each rat was individually placed into a cage for testing. The recorded time corresponded to the interval between the placement of the rat into the cage and the moment it successfully located the food lump. Each rat underwent two trials on the test day, at 10:00 and 16:00, respectively, and the average of the two results was calculated for data analysis.

Hematoxylin and Eosin Staining (HE)

After perfusion, the tissues were rapidly excised on ice and immediately immersed in 4% paraformaldehyde solution for fixation. Following fixation, the tissues were rinsed under running water for 2 hours to remove residual fixative. Subsequently, the tissues were dehydrated through a graded ethanol series (70%→80%→95%→100%) (#10092680, Sinopharm Group). Thereafter, the tissues were cleared twice in xylene for 10–15 minutes per cycle (#10023418, Sinopharm Group). The tissues were then infiltrated with paraffin wax in three successive baths for 0.5–1 hour each (#69018961, Sinopharm Group), embedded in paraffin, and sectioned at a thickness of 4–5 μm. The sections were floated and collected in a water bath, transferred onto glass slides, and dried at 60°C for 1–2 hours. The sections were dewaxed by immersion in xylene twice, each for 5–10 minutes, and rehydrated through a descending ethanol gradient (100%→95%→80%→70%→distilled water). Nuclear staining was performed using hematoxylin for 3–10 minutes (#H8070, Solarbio), followed by rinsing with tap water and differentiation with 1% acidic ethanol. The sections were subsequently rinsed under running water for 5–10 minutes to restore the hematoxylin staining color. Cytoplasmic staining was carried out with eosin for 1–5 minutes (#G1100, Solarbio). The sections were then dehydrated through an ascending ethanol gradient (70%→80%→95%→100%), cleared in xylene twice, and mounted with neutral gum (#G8590, Solarbio). Finally, the stained sections were examined under a light microscope.

Immunofluorescence

The tissue was fixed, embedded in wax, and sectioned. The sections were dewaxed to water and antigen retrieval was performed in a pressure cooker. Following this, the sections were blocked with 10% normal goat serum (#AR1009, Beijing Solarbio Science & Technology Co., Ltd) at 37°C for 1 hour and subsequently incubated overnight at 4°C with primary antibodies specific for CD86 (#bs-43589R, Beijing Bioss Biotechnology Co., Ltd., 1:1000) or CD206 (#bsm-60761R, Beijing Bioss Biotechnology Co., Ltd., 1:1000). After rinsing with PBS, the sections were incubated with fluorescent secondary antibodies (1:500) in the dark at room temperature for 1 hour. Finally, nuclei were stained with DAPI (#C1002, Beyotime) for 5–8 minutes, and the samples were visualized and imaged using a laser scanning confocal microscope.

Immunofluorescence Colocalization

The tissue was fixed, embedded in wax, and sectioned. The sections were dewaxed to water and antigen retrieval was performed in a pressure cooker. Following this, the sections were blocked with 10% normal goat serum (#AR1009, Beijing Solarbio Science & Technology Co., Ltd) at 37°C for 1 hour. Subsequently, the primary antibodies—TLR2 (#bs-10472R, Beijing Bioss Biotechnology Co., Ltd., 1:200) or GSDMD (#bs-14287R, Beijing Bioss Biotechnology Co., Ltd., 1:200)—were applied, and the sections were incubated at 4°C overnight. After thorough washing, the secondary antibody (1:400) was added, followed by incubation at room temperature in the dark for 1 hour. The sections were then washed again with PBS, and a second primary antibody, Iba-1 (#bs-1363R, Beijing Bioss Biotechnology Co., Ltd., 1:200), was applied for overnight incubation at 4°C. Following another washing step, the secondary antibody (1:400) was added and incubated at room temperature in the dark for 1 hour. Finally, the nuclei were stained with DAPI (#C1002, Beyotime), and the samples were examined and imaged using a laser scanning confocal microscope.

Western Blot

Following tissue extraction, samples were homogenized, lysed, and subsequently centrifuged. Protein concentration was measured using a BCA protein assay kit (Beyotime Biotechnology). An aliquot of 20–40 μg of total protein was resolved on a 12% SDS-PAGE gel and transferred onto a PVDF membrane (#IPVH00010, Millipore). The membrane was incubated overnight at 4°C with primary antibodies specific to TLR2 (#bs-1019R, Bioss, 1:1000), MyD88 (#bs-1047R, Bioss, 1:1000), p-NF-κB-p65 (#bs-7343R, Bioss, 1:1000), NLRP3 (#bs-41293R, Bioss, 1:1000), caspase-1 (#bsm-52441R, Bioss, 1:1000),

IL-1β (#bs-0812R, Bioss, 1:1000), and GSDMD (#bs-14287R, Bioss, 1:1000), followed by incubation with an IgG secondary antibody (#bs-10900R, Bioss, 1:5000) for 1 hour in the dark. Immunoreactive protein bands were visualized and quantified using an infrared fluorescence imaging system (LI-COR Biosciences, Lincoln, USA).

qRT-PCR

Total RNA was extracted using TRIzol reagent (#ER501-01, TRANS). The RNA was subsequently reverse transcribed into complementary cDNA using a reverse transcription kit (#AU341, TRANS). The mRNA expression levels of NLRP3 and GSDMD were quantified using SYBR Green Master Mix (#CW3008, Kangwei Century), with GAPDH serving as the internal reference gene (Table 1).

Statistical Analysis

SPSS 26.0 software was used. Data were presented as mean ± standard deviation. One-way ANOVA was used for comparison between groups. When variances were homogeneous, the LSD test was used; when variances were heterogeneous, the Dunnett's T3 test was used. $P<0.05$ was considered statistically significant.

Results

The Levels of DA and TH Gradually Decrease During the Progression of pPD

In this study, a rat model of pPD was established through a single-target injection of 6-OHDA into the striatum. Compared with the control group, the DA content in the 10 μg/4 μL, 13 μg/4 μL, and 16 μg/4 μL groups exhibited a progressive decline. Specifically, the striatal DA content was reduced by 30% to 40% in the 10 μg/4 μL group, 41% to 55% in the 13 μg/4 μL group, and 56% to 70% in the 16 μg/4 μL group (Figure 1A), effectively simulating the progressive pathological stages of pPD. Tyrosine hydroxylase (TH), which is expressed in the substantia nigra, serves as the rate-limiting enzyme in DA synthesis.[17] Compared with the control group, a gradual decrease in TH-positive neurons in the substantia nigra was observed in the 10 μg/4 μL, 13 μg/4 μL, and 16 μg/4 μL groups (Figure 1B and C). These findings indicate that a striatal injection of 6-OHDA at a dose of 10 μg/4 μL results in a 30% to 40% reduction in striatal DA content, corresponding to the pPD. During the pPD, as the dose of 6-OHDA increases, both DA content and TH expression progressively decline.

EA Can Improve the Non-Motor Symptoms in the pPD

The results of Result 3.1 demonstrated that the injection of 10 μg/4 μL of 6-OHDA into the striatum led to a 30% to 40% reduction in DA content, marking the entry into the pPD. It is widely recognized that pPD is characterized by various non-motor symptoms, including olfactory dysfunction, depression and anxiety, and sleep disturbances.[1] Therefore, this study aimed to evaluate the potential intervention effects of EA on these non-motor symptoms at this early stage. Compared with the control group, the model group exhibited a significantly reduced weight gain rate (Figure 2A), decreased sucrose preference (Figure 2B), prolonged immobility time in the tail suspension test (Figure 2C), increased sleep latency (Figure 2D), shortened sleep duration (Figure 2E), and prolonged time required to locate food (Figure 2F). After treatment with EA, the manifestations of the aforementioned non-motor symptoms were significantly improved.

Table 1 Primers Information

Gene Name	Forward Primer	Reverse Primer
NLRP3	5′-GGTTGGTGAATTCCGGCCTTACT-3′	5′-CTTACAGTCGGGGTGCAGAAGTC-3′
GSDMD	5′-TCCAGTGCCTCCATGAATGTGTG-3′	5′-TCACCATCTTCTTCCGGCTTTGG-3′
GAPDH	5′-GCCCAGAACATCATCCCTGCAT-3′	5′-GCCTGCTTCACCACCTTCTTGA-3′

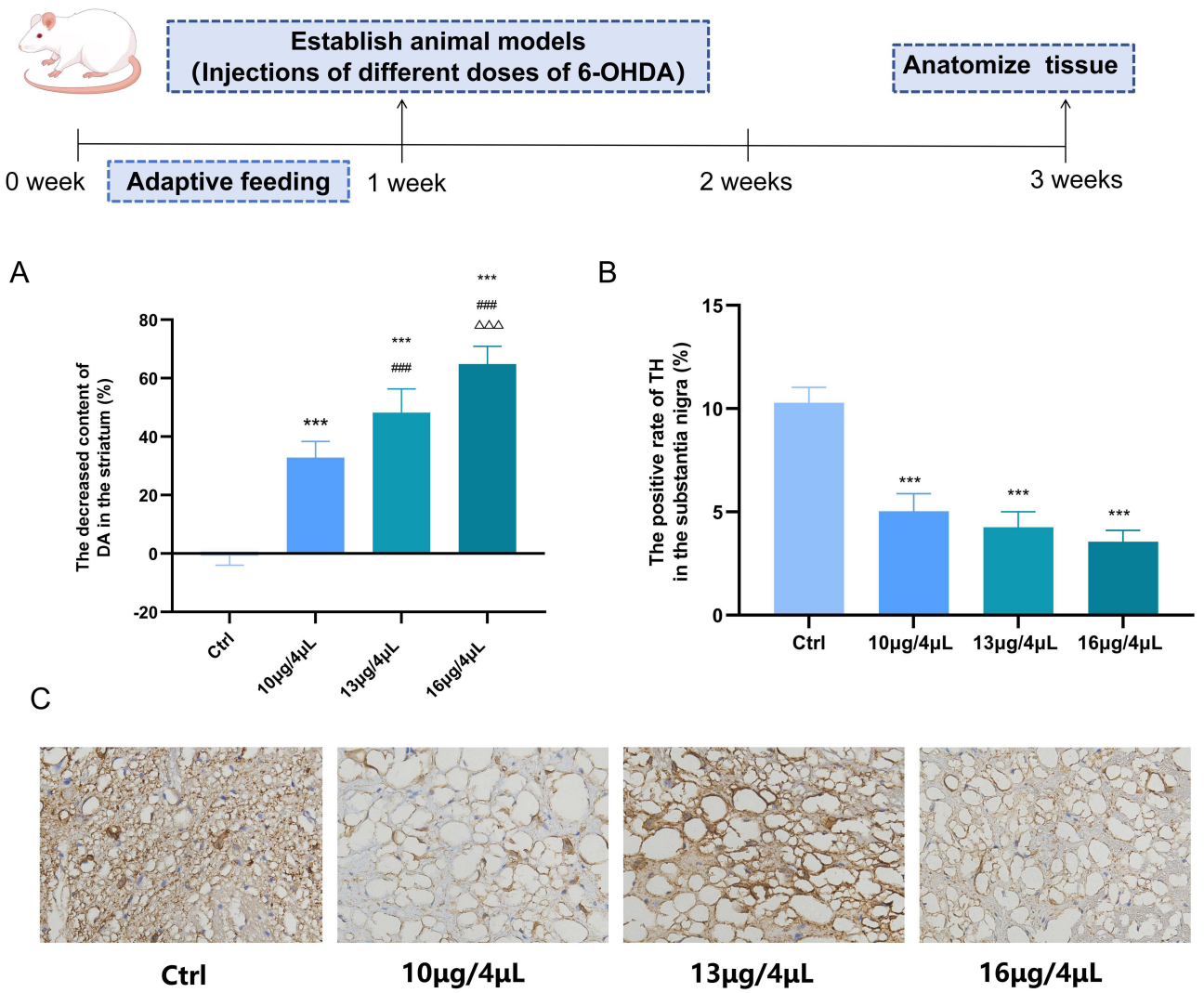

Figure 1 The levels of DA and TH gradually decrease during the progression of pPD. (**A**) ELISA was used to detect the reduction in striatal DA content caused by different doses of 6-OHDA. (**B** and **C**) ICH was used to detect the changes in TH positive rate in substantia nigra caused by different doses of 6-OHDA (magnification ×200, scale bar 50 μm).(n=3; compared with the control group, ***$P<0.001$; compared with the 10 μg/4 μL group, $^{###}P<0.001$; compared with the 13 μg/4 μL group, $^{\Delta\Delta\Delta}P<0.001$).

The Level of TLR2 Gradually Increases in Different Regions of pPD

TLR2, as a specific biomarker of pPD, may play a critical role in mediating neuroinflammatory processes associated with the disease. Therefore, we further examined the expression dynamics of TLR2 throughout the progression of pPD. Our findings revealed that, compared to the control group, TLR2 expression in the substantia nigra progressively increased in the 10 μg/4 μL, 13 μg/4 μL, and 16 μg/4 μL treatment groups (Figure 3A). In addition to the substantia nigra, the hippocampus, olfactory bulb, and colon are recognized as key pathological sites in pPD, which correspond to the non-motor symptoms such as depression, anxiety, olfactory dysfunction, and gastrointestinal disturbances. Accordingly, we extended our investigation to assess TLR2 expression in these regions. Our results demonstrated that TLR2 expression in the hippocampus (Figure 3B), olfactory bulb (Figure 3C), and colon (Figure 3D) exhibited a similar upward trend as observed in the substantia nigra. These findings suggest that as pPD progresses, TLR2 expression increases consistently across the substantia nigra, hippocampus, olfactory bulb, and colon. Therefore, TLR2 may significantly contribute to the progression of neuroinflammation in pPD. Based on this conclusion, we proceeded to investigate the mechanisms by which TLR2 mediates the exacerbation of neuroinflammation in pPD and evaluated the potential therapeutic effects of EA in subsequent experiments.

https://doi.org/10.2147/JIR.S585729

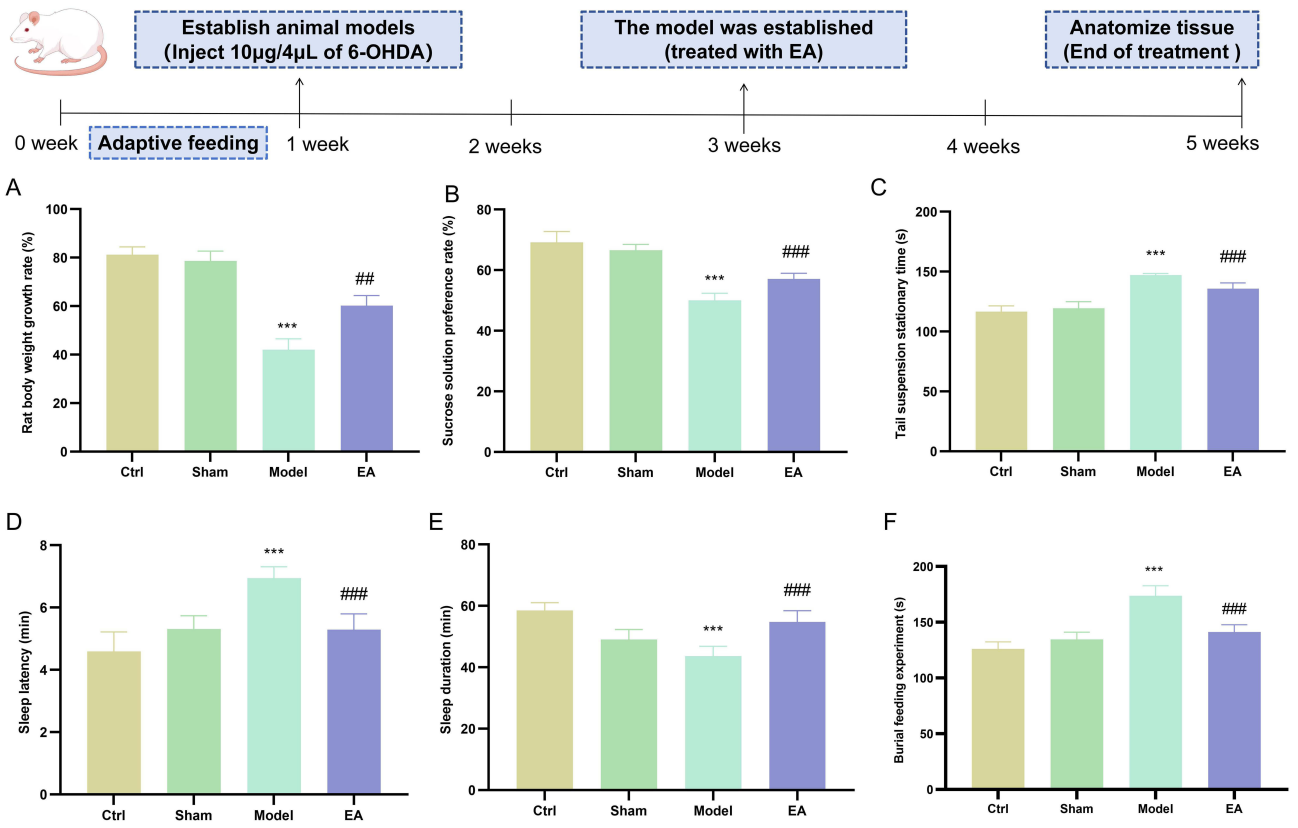

Figure 2 EA can improve the non-motor symptoms in the pPD. (**A**) Body weight growth rate in rats. (**B**) Sucrose preference rate in rats. (**C**) Tail suspension stationary time. (**D**) Sleep latency. (**E**) Sleep duration. (**F**) Burial food experiment. (n=6; compared with the control group, ***P<0.001; compared with the model group, ###P<0.001,##P<0.01).

EA Can Inhibit the Activation of Microglia in pPD

Result 3.2 demonstrated the significant therapeutic effect of EA on pPD, and Result 3.3 confirmed the progressive development of neuroinflammation in pPD. Pathological neuroinflammation associated with neurodegeneration is primarily mediated by microglia, which are the resident immune cells of the central nervous system (CNS).[18] Therefore, we further examined microglial activation in pPD and the regulatory effects of EA. The study revealed that, compared with the control group, the CD86-positive area in the model group was significantly increased (Figure 4A and C), while the CD206-positive area was significantly decreased (Figure 4B and D). This situation was significantly reversed after EA treatment. After EA treatment, it promoted the transformation of microglia from the pro-inflammatory M1 type to the anti-inflammatory M2 type, and inhibited the activation of pPD microglia.

EA Can Inhibit the Activation of Microglia in the pPD Stage Mediated by TLR2

Result 3.4 demonstrated that microglial activation occurs in the pPD model, and that EA can effectively suppress this activation. Result 3.3 focused on the expression of TLR2 in pPD. Based on these findings, we hypothesized that TLR2 may play a mediating role in microglial activation during pPD. To test this hypothesis, we performed immunofluorescence co-localization analysis to assess the spatial relationship between TLR2 and Iba-1, a specific microglial marker. Our results revealed a significant increase in the co-localization area of TLR2 and Iba-1 in the Model group compared to the control group. This increase was markedly reduced following treatment in the EA group (Figure 5A and B). Additionally, HE staining was conducted to evaluate inflammatory infiltration and neuronal necrosis in the substantia nigra. The results confirmed that the model group exhibited significant inflammatory infiltration and neuronal necrosis in the substantia nigra compared to the control group, and these pathological changes were notably ameliorated following EA treatment (Figure 5C). Taken together, these findings suggest that TLR2 mediates microglial activation during the

https://doi.org/10.2147/JIR.S585729

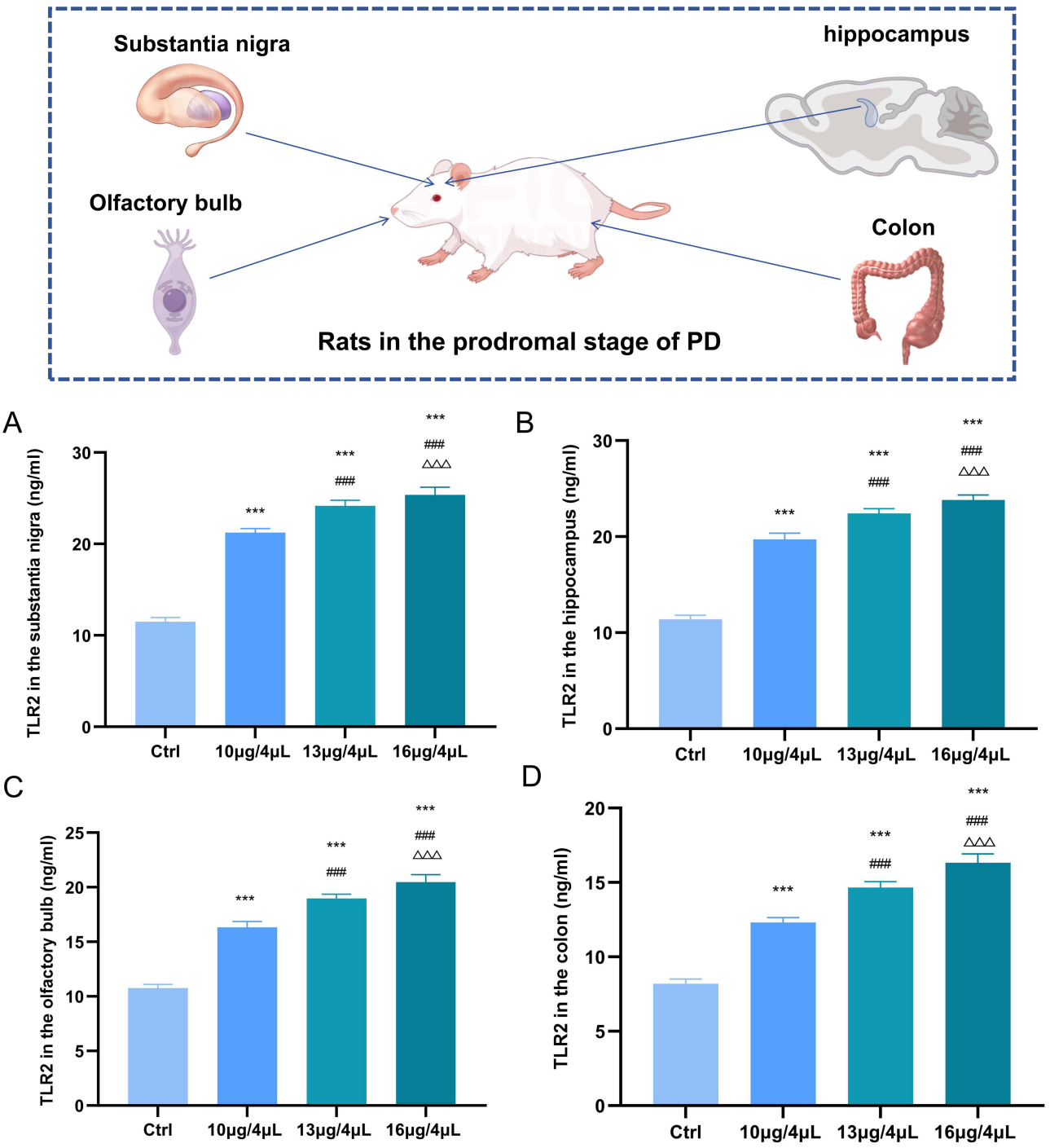

Figure 3 The level of TLR2 gradually increases in different regions of pPD. (**A**) TLR2 levels in the substantia nigra of pPD were detected by ELISA. (**B**) TLR2 levels in the hippocampus of pPD were detected by ELISA. (**C**) TLR2 levels in the olfactory bulb of pPD were detected by ELISA. (**D**) TLR2 levels in the colon of pPD were detected by ELISA. (n=3; compared with the control group, $^{***}P<0.001$; compared with the 10 μg/4 μL group, $^{\#\#\#}P<0.001$; compared with the 13 μg/4 μL group, $^{\Delta\Delta\Delta}P<0.001$).

pPD, accompanied by evident inflammatory infiltration and neuronal damage in the substantia nigra. EA demonstrates a significant inhibitory effect on these pathological processes.

EA Can Inhibit the Activation of the TLR2/NF-κB/NLRP3 Pathway in the pPD

Based on previous research, we observed that EA treatment could suppress TLR2-mediated neuroinflammation in pPD. Therefore, we further examined the classical TLR2 inflammatory signaling pathway, specifically the TLR2/NF-κB/

https://doi.org/10.2147/JIR.S585729

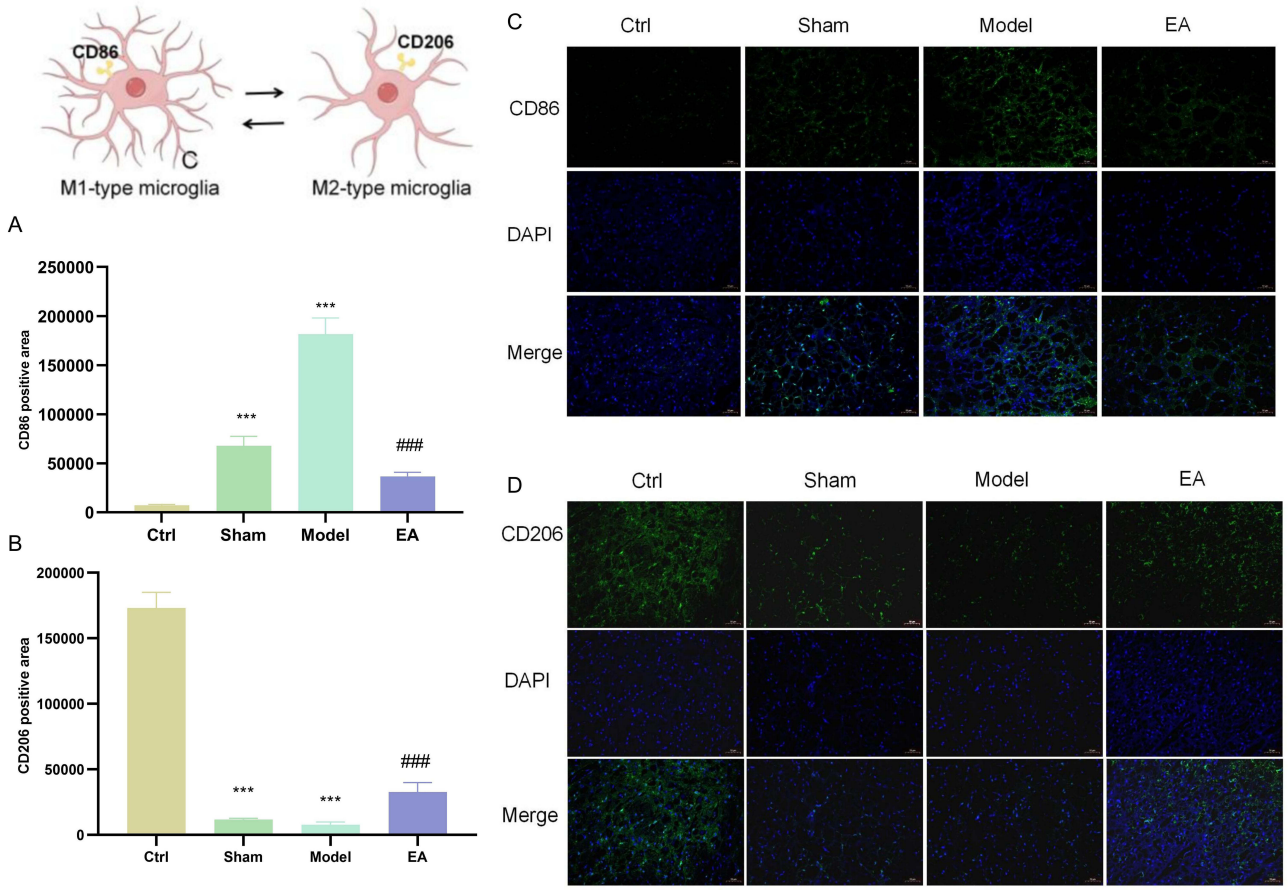

Figure 4 EA can inhibit the activation of microglia in pPD. (**A** and **B**) Positive area of CD86, a pro-inflammatory marker of M1-type microglia in substantia nigra, detected by immunofluorescence. (**C** and **D**) Positive area of CD206, an anti-inflammatory marker of M2-type microglia in substantia nigra, detected by immunofluorescence. (Magnification ×200, scale bar 50 μm). (n=3; compared with the control group, ***P<0.001; compared with the model group, ###P<0.001).

NLRP3, and evaluated the expression levels of downstream proteins including Caspase-1, GSDMD, and IL-1β. Compared with the control group, the model group exhibited significantly elevated protein expression levels of TLR2 (Figure 6A), MyD88 (Figure 6B), p-NF-κB-p65 (Figure 6C), NLRP3 (Figure 6D), Caspase-1 (Figure 6E), GSDMD (Figure 6F), and IL-1β (Figure 6G). Following treatment in the EA group, these elevated expression levels were markedly reduced.

EA Inhibits Microglial Pyroptosis in the pPD

Based on the findings of Result 3.6, we observed alterations in the protein expressions of Caspase-1, IL-1β, and GSDMD, which are downstream effectors of NLRP3. These proteins are closely associated with pyroptosis, a form of programmed cell death accompanied by intense inflammatory responses. Upon activation, NLRP3 initiates the assembly of the inflammasome complex, leading to the maturation of caspase-1, which subsequently activates IL-1β and cleaves GSDMD. This cascade ultimately results in plasma membrane rupture and the induction of pyroptosis.[19] Therefore, we further examined the mRNA expression levels of NLRP3 and GSDMD during the pPD. Compared to the control group, the model group exhibited significantly elevated mRNA levels of both NLRP3 and GSDMD. These increases were attenuated following treatments in the EA group (Figure 7A and B).

GSDMD serves as the key effector protein in pyroptosis. To determine the cellular localization of pyroptosis, we performed immunofluorescence co-localization analysis using the microglial cell surface marker Iba-1 and GSDMD (Figure 7C and D). Compared with the control group, the co-localization area was significantly increased in the model group. This increase was attenuated following treatment with EA. These findings suggest that in pPD, EA suppresses the

https://doi.org/10.2147/JIR.S585729

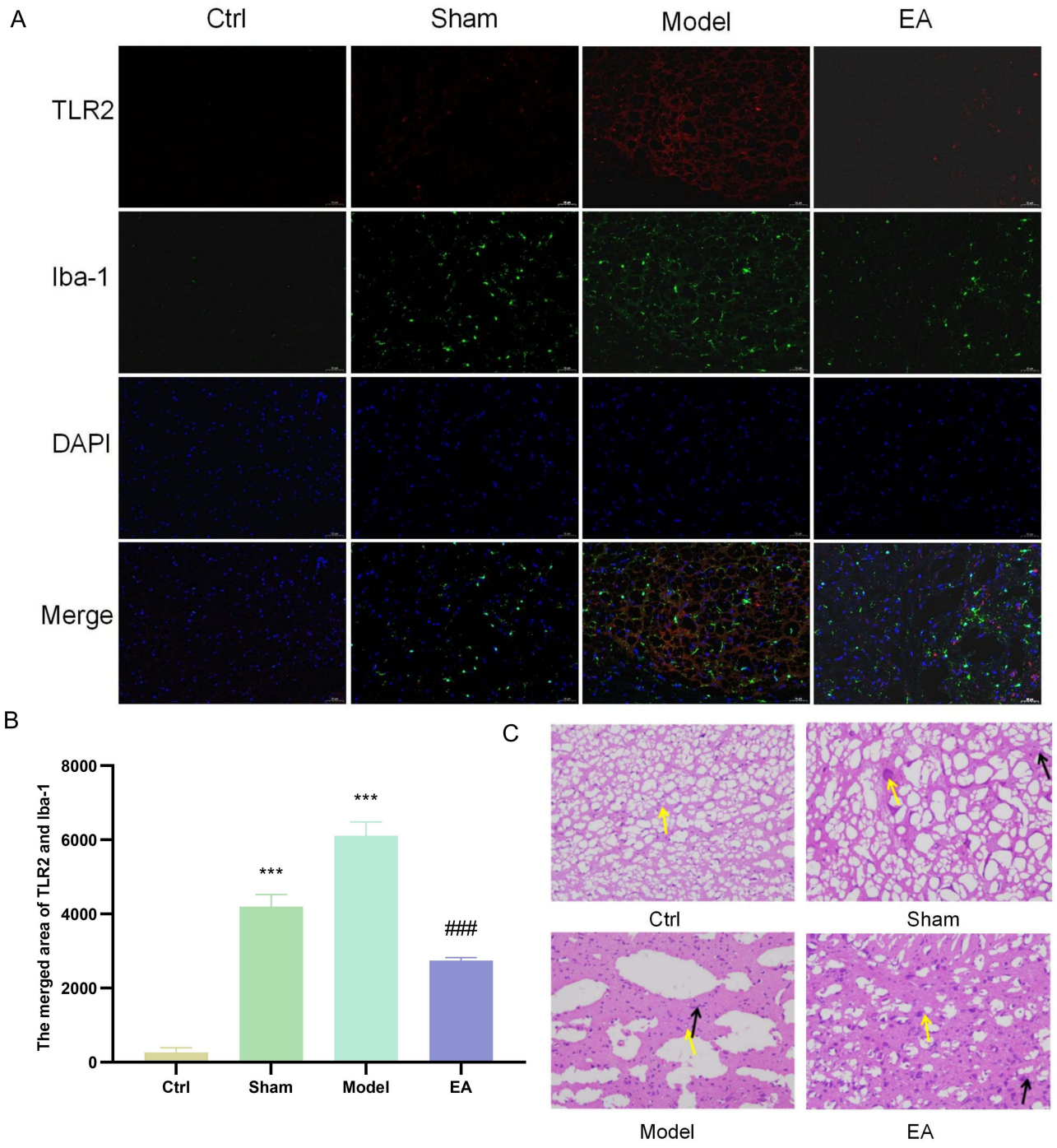

Figure 5 EA can inhibit the activation of microglia in the pPD stage mediated by TLR2. (**A** and **B**) Immunofluorescence co-localization was used to detect the co-localization area of TLR2 in substantia nigra and the surface marker Iba-1 of microglia (magnification ×200, scale bar 50 μm). (**C**) HE staining of substantia nigra, yellow arrows indicate neuronal necrosis, and black arrows indicate inflammatory infiltration.(n=3; compared with the control group, $^{***}P<0.001$; compared with the model group, $^{\#\#\#}P<0.001$).

expression of pyroptosis-related genes, specifically NLRP3 and GSDMD mRNA. Furthermore, our study demonstrates that pyroptosis occurs in microglial cells, and EA exerts an inhibitory effect on pyroptosis within these cells. This provides additional evidence that a robust inflammatory response is involved in pPD, and EA can effectively mitigate this inflammatory activity.

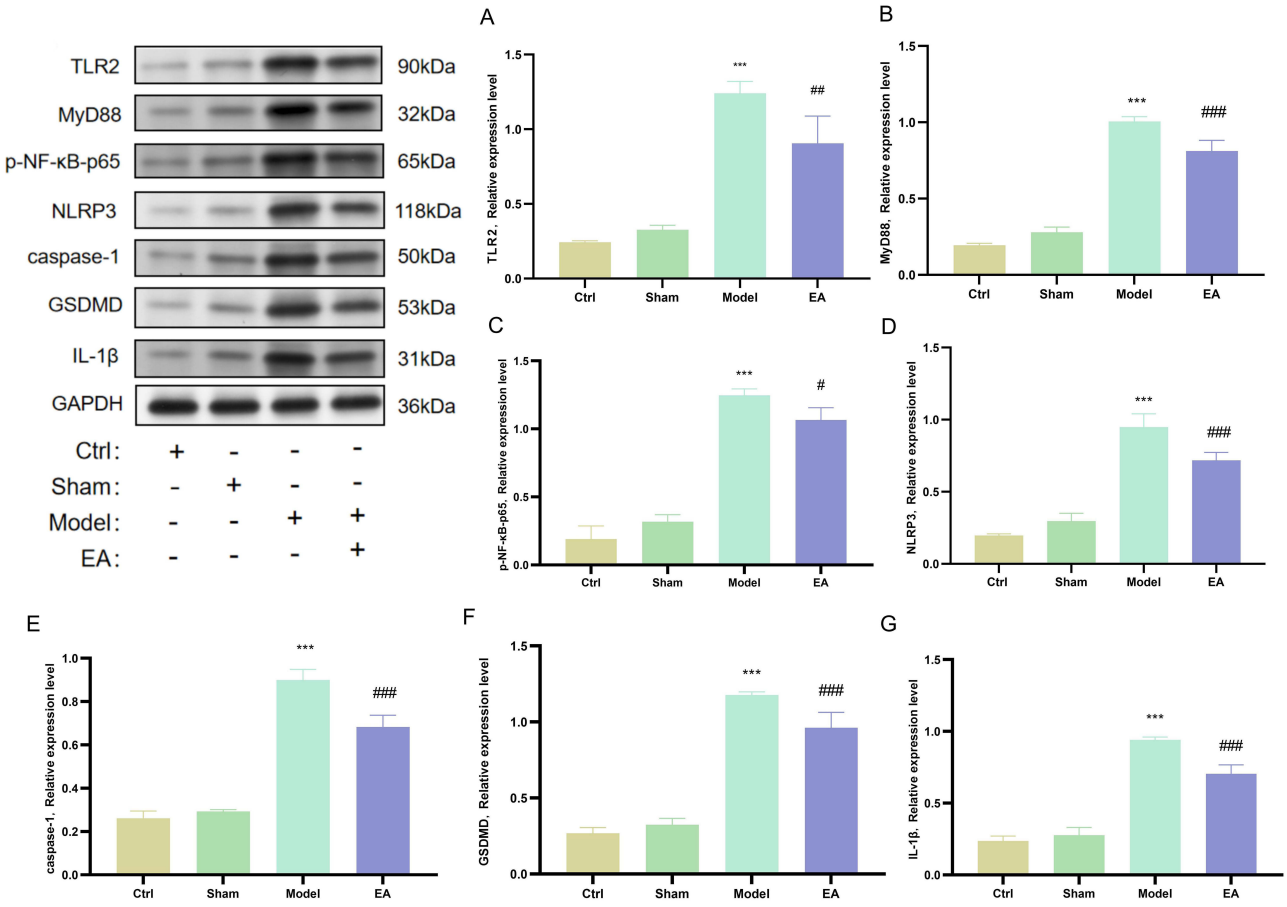

Figure 6 EA can inhibit the activation of microglia in the pPD stage mediated by TLR2. (**A**) Western blot detection of TLR2 protein expression in the substantia nigra. (**B**) Western blot detection of MyD88 protein expression in the substantia nigra. (**C**) Western blot detection of p-NF-κB-p65 expression in the substantia nigra. (**D**) Western blot detection of NLRP3 protein expression in the substantia nigra. (**E**) Western blot detection of Caspase-1 protein expression in the substantia nigra. (**F**) Western blot detection of GSDMD protein expression in the substantia nigra. (**G**) Western blot detection of IL-1β protein expression in the substantia nigra. (n=6; compared with the control group, ***P<0.001; compared with the model group, $^{###}P$<0.001, $^{##}P$<0.01, $^{#}P$<0.05).

Discussion

Since the initial report of using 6-OHDA to establish a rat model in 1968, the administration of catecholamine neurotoxins to mimic the depletion of DA in the nigrostriatal pathway in PD has become a widely accepted method. 6-OHDA exhibits a remarkably high affinity for the DA transporter. When stereotactically injected into the striatum of rodents, it triggers progressive neurodegeneration within the nigrostriatal pathway, resulting in substantial neuronal damage and DA depletion.[20] The advantage of unilateral striatal injection of 6-OHDA lies in its ability to induce a progressive loss of dopaminergic neurons and localized pathological changes, closely resembling the pathophysiological progression of PD. Moreover, the relatively large size of the rat striatum contributes to a higher success rate in model establishment.[21] Following the injection of 4 μg of 6-OHDA into the unilateral striatum, partial degeneration of the nigrostriatal pathway can typically be observed approximately two weeks later.[22] During this period, behavioral impairments gradually stabilize, accompanied by characteristic pathological alterations in the basal ganglia nuclei. Typically, behavioral assessments are conducted between 14 and 21 days post-lesion surgery, at which point DA depletion has reached its peak and stabilized.[23] Therefore, this method demonstrates the reliability of using unilateral striatal injections of varying doses of 6-OHDA to simulate the pathological progression of PD.

EA represents a highly promising approach within traditional Chinese medicine for the treatment of neurological disorders. Our research group previously demonstrated that the acupuncture technique of "Tiao Shen Chang Zhi" significantly improves motor symptoms in PD.[24] It is well established that the pPD stage is associated with various non-motor symptoms, including olfactory dysfunction, anxiety and depression, and sleep disturbances. The findings of this

https://doi.org/10.2147/JIR.S585729

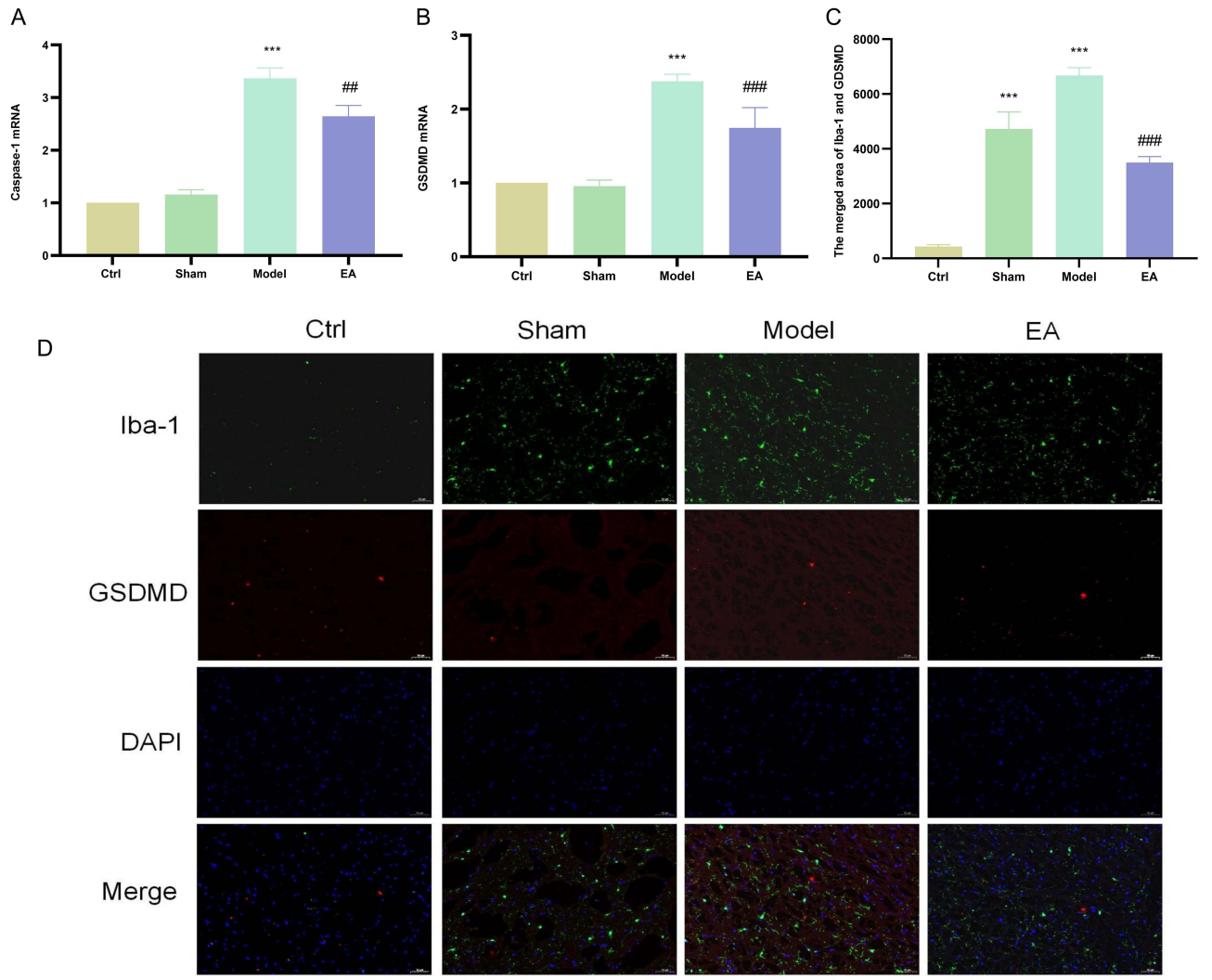

Figure 7 EA inhibits microglial pyroptosis in the pPD. (**A**) qRT-PCR was used to detect NLRP3 mRNA in the substantia nigra. (**B**) qRT-PCR was used to detect GSDMD mRNA in the substantia nigra. (**C** and **D**) Co-localization of Iba-1 and GSDMD in the substantia nigra was detected by immunofluorescence co-localization (magnification ×200, scale bar 50 μm). (n=3; compared with the control group, ***P<0.001; compared with the model group, ###P<0.001, ##P<0.01).

study indicate that EA treatment significantly enhances body weight gain, sucrose preference, and total sleep duration in pPD rats, while reducing tail suspension time, food-seeking latency, and sleep latency. This study further confirms that the injection of 10 μg/4 μL of 6-OHDA into the striatum, resulting in a 30–40% loss of DA, successfully induces the prodromal phase, accompanied by prominent non-motor symptoms. Notably, EA, as a promising integrative therapeutic strategy, demonstrates significant efficacy in ameliorating non-motor symptoms such as olfactory dysfunction, mood disorders, and sleep disturbances in pPD.

Toll-like receptors are type I transmembrane proteins capable of activating the innate immune response by recognizing and binding to specific molecular patterns.[25] Karlijn's team performed autopsies on the brains of deceased patients, and their study was the first to confirm the involvement of TLR2 in neuroinflammatory responses in the human brain during the pPD.[5] Given that other subtypes of the Toll family do not elicit this effect, the TLR2 subtype is considered highly specific in pPD. Our study further investigates this phenomenon in a more comprehensive and detailed manner. The substantia nigra, hippocampus, olfactory bulb, and colon are recognized as key pathological sites in pPD and are closely associated with non-motor symptoms such as olfactory dysfunction, anxiety and depression, cognitive impairment, and constipation.[26–31] Our findings indicate that, first, as pPD progresses, the levels of TLR2-mediated neuroinflammation in these four regions gradually increase, demonstrating that neuroinflammation in pPD is a continuously progressing process. Second, across all individual stages of pPD, the

expression levels of TLR2 exhibit a consistent pattern: the highest expression is observed in the substantia nigra, followed by the hippocampus and olfactory bulb, with the lowest levels detected in the colon. Further analysis suggests that this pattern may be attributable to the experimental model used in our study, which involves the intrastriatal injection of 6-OHDA. Factors such as the diffusion rate of the neurotoxin and the spatial distances between regions may contribute to the observed trend in TLR2 expression levels across stages. Nevertheless, the results of our study unequivocally confirm that TLR2-mediated neuroinflammation progresses continuously throughout the course of pPD.

Toll-like receptors can activate immune responses in the CNS through mechanisms such as mediating neuroinflammation and activating microglia, particularly in neurodegenerative diseases such as PD.[32,33] Pathological neuroinflammation associated with neurodegeneration is primarily mediated by microglia, which are the resident immune cells of the CNS.[34] Our research revealed that in the pPD model group, the expression of the M1 pro-inflammatory marker CD86[35] in microglia was increased, whereas the expression of the M2 anti-inflammatory marker CD206[36] was reduced, indicating that microglia were in an activated state, and this activation was reversed following treatment in the EA group. Furthermore, immunofluorescence-based co-localization analysis of TLR2 and the microglial surface marker Iba-1[37] confirmed that TLR2 mediated microglial activation during this stage of pPD, and EA treatment significantly suppressed this activation. Additionally, histopathological analysis via HE staining further demonstrated the presence of inflammatory infiltration and neuronal necrosis in the substantia nigra of pPD, both of which were markedly attenuated following EA treatment.

The TLR2/NF-κB/NLRP3 represents a classical inflammatory signaling pathway mediated by TLR2.[6,32,38] In this study, we assessed the expression levels of key molecules along this pathway, including TLR2, MyD88, p-NF-κB-p65, and NLRP3. Additionally, we evaluated the expression of downstream effectors of NLRP3, namely Caspase-1, IL-1β, and GSDMD. Our results demonstrated that the expression levels of TLR2, MyD88, p-NF-κB-p65, and NLRP3 were significantly elevated in the model group. However, these increases were attenuated following treatment in the EA group. Similarly, the expression levels of Caspase-1, IL-1β, and GSDMD followed the same trend.

Our previous study demonstrated that the expression levels of Caspase-1, IL-1β, and GSDMD, which are downstream effectors of NLRP3, were altered. NLRP3, Caspase-1, IL-1β, and GSDMD are well-established biomarkers associated with pyroptosis.[39–41] Therefore, we further examined the mRNA expression levels of NLRP3 and GSDMD, which exhibited a consistent trend. The expression levels increased in the model group, whereas treatment with EA reversed this trend, which exhibited the most significant therapeutic effect. Among these markers, GSDMD serves as the terminal effector protein in pyroptosis; its N-terminal fragment (GSDMD-N) can bind to membrane lipids, disrupt membrane integrity, and ultimately lead to cell membrane rupture and pyroptotic cell death.[42] To further investigate the cellular localization of pyroptosis, we employed immunofluorescence co-localization analysis of Iba-1 and GSDMD. As pyroptosis is characterized by a robust inflammatory response, our findings confirm that pyroptosis occurs in the context of pPD, specifically within microglial cells. Moreover, our results indicate that EA exerts an inhibitory effect on microglial pyroptosis.

This study concludes (Figure 8) that the injection of 10 μg/4 μL of 6-OHDA into the striatum results in a 30% to 40% reduction in DA content, marking the onset of the pPD. During this stage, non-motor symptoms such as olfactory dysfunction, depression, anxiety, and sleep disturbances begin to manifest. Administration of EA demonstrates significant therapeutic potential in alleviating these non-motor symptoms. TLR2 exhibits high specificity in pPD, with a progressive increase in TLR2-mediated neuroinflammation observed in the substantia nigra, hippocampus, olfactory bulb, and colon. Under pathological conditions, TLR2 contributes to microglial activation in pPD, triggering the TLR2/NF-κB/NLRP3 signaling pathway and inducing microglial pyroptosis. EA can intervene in the series of early neuroinflammatory cascades mediated by TLR2 during the pPD stage. Therefore, EA is expected to become a potential therapy for preventing pPD from further developing into PD.

However, this study has certain limitations. The 6-OHDA model we used cannot fully simulate the disease progression of pPD. It can only represent a portion of sporadic PD. In the future, we will combine A53T mice to conduct research on the disease progression of the pre-disease stage of genotype PD.

https://doi.org/10.2147/JIR.S585729

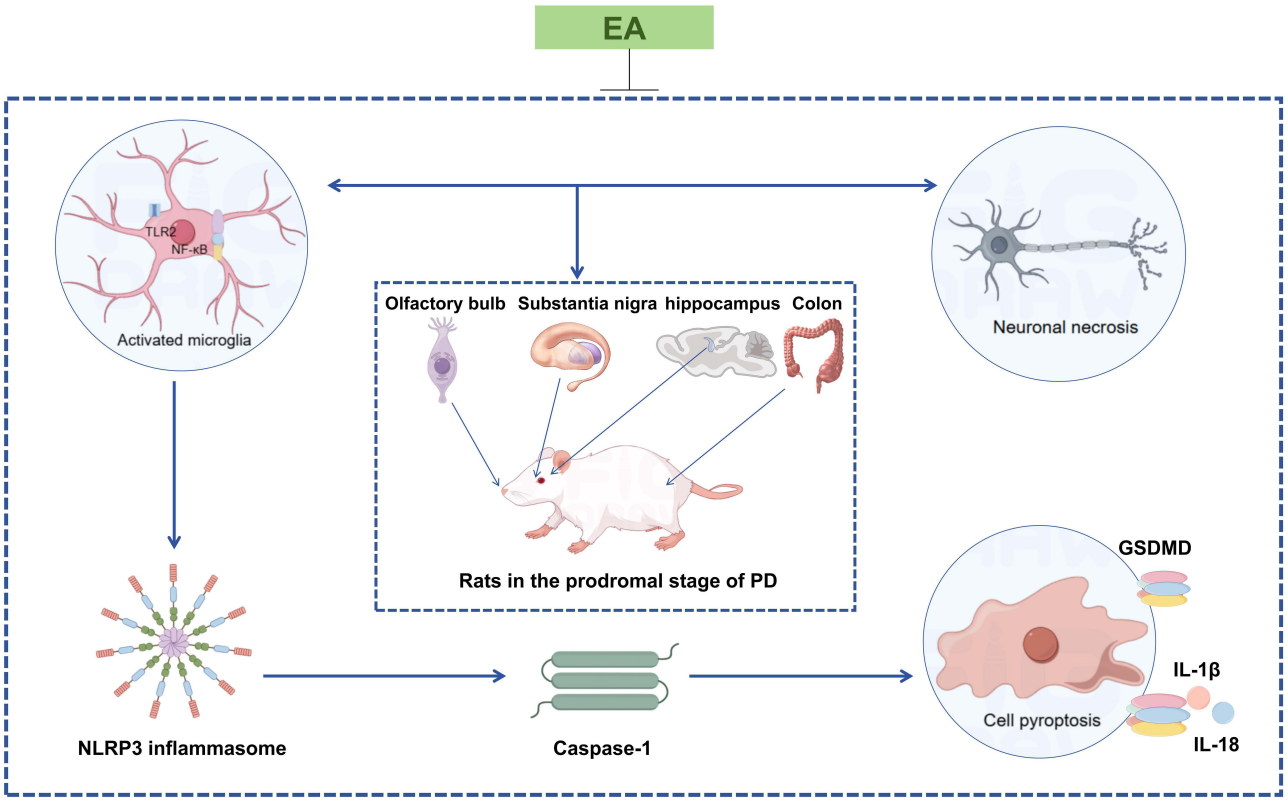

Figure 8 EA intervention affects the expression of TLR2 in different regions of pPD, inhibits microglial activation, regulates the TLR2/NF-κB/NLRP3 pathway, and suppresses pyroptosis of microglia.

Abbreviations

pPD, The prodromal period of Parkinson's disease; PD, Parkinson's disease; TLR2, toll-like receptor 2; DA, dopamine; PET, positron emission tomography; α-Syn, α-synuclein; EA, electroacupuncture; TH, Tyrosine hydroxylase; CNS, central nervous system.

Ethics Approval

We confirm that this manuscript is original, has not been published previously, and is not currently under consideration for publication elsewhere. We also confirm that the animal experiments were conducted in accordance with international animal protection guidelines and approved by the Ethics Committee of Heilongjiang University of Chinese Medicine (No. 2023122908). We confirm that this animal research complies with the requirements of the "ARRIVE" animal welfare guidelines.

Author Contributions

KX - Investigation, Project administration, Writing - original draft. YL - Methodology, Visualization. BCH - Resources, Software. YZ - Data curation, Formal analysis. YB - Supervision, Validation. SW - Conceptualization, Funding acquisition, Writing - review & editing. All authors took part in drafting, revising or critically reviewing the article; gave final approval of the version to be published; have agreed on the journal to which the article has been submitted; and agree to be accountable for all aspects of the work.

Funding

This research was supported by the National Natural Science Foundation of China (82474664) and the Scientific Research Business Expenses Project Task Book of Provincial Research Institutes in Heilongjiang Province (CZKYF2020B003).

Disclosure

The authors declare that they have no known competing financial interests or personal relationships that could have appeared to influence the work reported in this paper.

References

1. Boura I, Poplawska-Domaszewicz K, Limbachiya N, Trivedi D, Batzu L, Chaudhuri KR. Prodromal Parkinson's disease: a snapshot of the landscape. *Neurol Clin*. 2025;43(2):209–228. doi:10.1016/j.ncl.2024.12.004
2. Filimontseva A, Fu Y, Vila M, Halliday GM. Neuromelanin and selective neuronal vulnerability to Parkinson's disease. *Trends Neurosci*. 2025;48(6):445–459. doi:10.1016/j.tins.2025.04.005
3. Hilker R, Schweitzer K, Coburger S, et al. Nonlinear progression of Parkinson disease as determined by serial positron emission tomographic imaging of striatal fluorodopa F 18 activity. *Arch Neurol*. 2005;62(3):378–382. doi:10.1001/archneur.62.3.378
4. Pradhan S, Andreasson K. Commentary: progressive inflammation as a contributing factor to early development of Parkinson's disease. *Exp Neurol*. 2013;241:148–155. doi:10.1016/j.expneurol.2012.12.008
5. Doorn KJ, Moors T, Drukarch B, van de Berg W, Lucassen PJ, van Dam AM. Microglial phenotypes and toll-like receptor 2 in the substantia nigra and hippocampus of incidental Lewy body disease cases and Parkinson's disease patients. *Acta Neuropathol Commun*. 2014;2:90. doi:10.1186/s40478-014-0090-1
6. Yang L, Mao K, Yu H, Chen J. Neuroinflammatory responses and Parkinson' disease: pathogenic mechanisms and therapeutic targets. *J Neuroimmune Pharmacol*. 2020;15(4):830–837. doi:10.1007/s11481-020-09926-7
7. Liu F, Liu ZB, Ma X, Wang Q, Wang Y. Effect of electroacupuncture on brain-gut oxidative stress in Parkinson's disease mice. *Zhen Ci Yan Jiu*. 2024;49(3):256–264. doi:10.13702/j.1000-0607.20230515
8. Xin YY, Wang JX, Xu AJ. Electroacupuncture ameliorates neuroinflammation in animal models. *Acupunct Med*. 2022;40(5):474–483. doi:10.1177/09645284221076515
9. Pak ME, Ahn SM, Jung DH, et al. Electroacupuncture therapy ameliorates motor dysfunction via brain-derived neurotrophic factor and glial cell line-derived neurotrophic factor in a mouse model of Parkinson's disease. *J Gerontol a Biol Sci Med Sci*. 2020;75(4):712–721. doi:10.1093/gerona/glz256
10. Lyu P, Wen F, Fu Z, et al. Electroacupuncture regulates mitochondria-endoplasmic reticulum interactions via Fn1 in a Parkinson's disease model: transcriptomic evidence. *J Integr Neurosci*. 2025;24(9):40105. doi:10.31083/jin40105
11. Geng X, Zou Y, Huang T, Li S, Pang A, Yu H. Electroacupuncture improves neuronal damage and mitochondrial dysfunction through the TRPC1 and SIRT1/AMPK Signaling pathways to alleviate Parkinson's disease in mice. *J Mol Neurosci*. 2024;74(1):5. doi:10.1007/s12031-023-02186-z
12. Hsu WT, Chen YH, Yang HB, Lin JG, Hung SY. Electroacupuncture improves motor symptoms of Parkinson's disease and promotes neuronal autophagy activity in mouse brain. *Am J Chin Med*. 2020;48(7):1651–1669. doi:10.1142/s0192415x20500822
13. Quan J, Liu X, Liang S, et al. Electroacupuncture suppresses motor impairments via microbiota-metabolized LPS/NLRP3 signaling in 6-OHDA induced Parkinson's disease rats. *Int Immunopharmacol*. 2025;162:115089. doi:10.1016/j.intimp.2025.115089
14. Tang X, Wang C, Tian S, Wen H, Zhang H. Acupuncture for neurodegenerative diseases: mechanisms, efficacy, and future research directions. *Am J Transl Res*. 2025;17(5):3703–3717. doi:10.62347/qfjo6227
15. Wang M, Zheng HS, Ye WL, et al. The mechanism of electroacupuncture-mediated improvement in Parkinson's disease by inhibiting ferroptosis through activating the Nrf2/GPX4 signal pathway. *Front Aging Neurosci*. 2025;17:1551404. doi:10.3389/fnagi.2025.1551404
16. Pereira CR, Machado J, Criado B, et al. Analysis of patellar reflex in Parkinson disease patients after an acupuncture treatment protocol - case series study. *Clin Park Relat Disord*. 2025;12:100324. doi:10.1016/j.prdoa.2025.100324
17. Ugrumov MV. Hypothalamic neurons fully or partially expressing the dopaminergic phenotype: development, distribution, functioning and functional significance. A review. *Front Neuroendocrinol*. 2024;75:101153. doi:10.1016/j.yfrne.2024.101153
18. Dalla Verde C, Jayanti S, El Khobar K, Stanford JA, Tiribelli C, Gazzin S. Understanding the pre-clinical stages of Parkinson's disease: where are we in clinical and research settings? *Int J Mol Sci*. 2025;26(14). doi:10.3390/ijms26146881
19. Liu T, Kong X, Qiao J, Wei J. Decoding Parkinson's disease: the interplay of cell death pathways, oxidative stress, and therapeutic innovations. *Redox Biol*. 2025;85:103787. doi:10.1016/j.redox.2025.103787
20. Blandini F, Levandis G, Bazzini E, Nappi G, Armentero MT. Time-course of nigrostriatal damage, basal ganglia metabolic changes and behavioural alterations following intrastriatal injection of 6-hydroxydopamine in the rat: new clues from an old model. *Eur J Neurosci*. 2007;25(2):397–405. doi:10.1111/j.1460-9568.2006.05285.x
21. Jankovic J, Tan EK. Parkinson's disease: etiopathogenesis and treatment. *J Neurol Neurosurg Psychiatry*. 2020;91(8):795–808. doi:10.1136/jnnp-2019-322338
22. Chen F, Shi L, Xie J. motor and anxiety symptoms in a mouse model of 6-hydroxydopamine-induced Parkinson's disease. *J Qingdao Univ*. 2023;50(03):321–324.
23. Orieux G, Francois C, Féger J, et al. Metabolic activity of excitatory parafascicular and pedunculopontine inputs to the subthalamic nucleus in a rat model of Parkinson's disease. *Neuroscience*. 2000;97(1):79–88. doi:10.1016/s0306-4522(00)00011-7
24. Li Y, Zhu J, Sang P, et al. Effect of Tiaoshen Changzhi acupuncture on behavior and striatum ΔFosB in rats with levodopa-induced dyskinesias. *Biotechnol Genet Eng Rev*. 2024;40(4):3916–3930. doi:10.1080/02648725.2023.2204694
25. Maihemuti N, Shi Y, Zhang K, et al. Toll-like receptors in the immunotherapy era: dual-edged swords of tumor immunity and clinical translation. *MedComm*. 2025;6(8):e70308. doi:10.1002/mco2.70308
26. Wakabayashi K. Where and how alpha-synuclein pathology spreads in Parkinson's disease. *Neuropathology*. 2020;40(5):415–425. doi:10.1111/neup.12691
27. Baltazar MT, Dinis-Oliveira RJ, de Lourdes Bastos M, Tsatsakis AM, Duarte JA, Carvalho F. Pesticides exposure as etiological factors of Parkinson's disease and other neurodegenerative diseases–a mechanistic approach. *Toxicol Lett*. 2014;230(2):85–103. doi:10.1016/j.toxlet.2014.01.039
28. Li SJ, Lo YC, Tseng HY, et al. Nucleus accumbens deep brain stimulation improves depressive-like behaviors through BDNF-mediated alterations in brain functional connectivity of dopaminergic pathway. *Neurobiol Stress*. 2023;26:100566. doi:10.1016/j.ynstr.2023.100566

29. Li K, Yan L, Zhang Y, et al. Seahorse treatment improves depression-like behavior in mice exposed to CUMS through reducing inflammation/oxidants and restoring neurotransmitter and neurotrophin function. *J Ethnopharmacol*. 2020;250:112487. doi:10.1016/j.jep.2019.112487
30. Tian G, Wang B, Kong B, et al. Stereoscopic quantitative analysis of enteric nervous system in patients with slow transit constipation. *Neurogastroenterol Motil*. 2025;37(12):e70128. doi:10.1111/nmo.70128
31. Han B, Jiang W, Liu H, et al. Upregulation of neuronal PGC-1α ameliorates cognitive impairment induced by chronic cerebral hypoperfusion. *Theranostics*. 2020;10(6):2832–2848. doi:10.7150/thno.37119
32. Heidari A, Yazdanpanah N, Rezaei N. The role of Toll-like receptors and neuroinflammation in Parkinson's disease. *J Neuroinflammation*. 2022;19(1):135. doi:10.1186/s12974-022-02496-w
33. Choi I, Zhang Y, Seegobin SP, et al. Microglia clear neuron-released α-synuclein via selective autophagy and prevent neurodegeneration. *Nat Commun*. 2020;11(1):1386. doi:10.1038/s41467-020-15119-w
34. Rodríguez-Gómez JA, Kavanagh E, Engskog-Vlachos P, et al. Microglia: agents of the CNS pro-inflammatory response. *Cells*. 2020;9(7). doi:10.3390/cells9071717
35. Colonna M, Butovsky O. Microglia function in the central nervous system during health and neurodegeneration. *Annu Rev Immunol*. 2017;35:441–468. doi:10.1146/annurev-immunol-051116-052358
36. Kitaoka S. Microglia regulate neuronal and behavioural functions under physiological and pathological conditions. *J Biochem*. 2023;173(3):153–157. doi:10.1093/jb/mvac099
37. Hoogland IC, Houbolt C, van Westerloo DJ, van Gool WA, van de Beek D. Systemic inflammation and microglial activation: systematic review of animal experiments. *J Neuroinflammation*. 2015;12:114. doi:10.1186/s12974-015-0332-6
38. Kouli A, Horne CB, Williams-Gray CH. Toll-like receptors and their therapeutic potential in Parkinson's disease and α-synucleinopathies. *Brain Behav Immun*. 2019;81:41–51. doi:10.1016/j.bbi.2019.06.042
39. Huang Y, Xu W, Zhou R. NLRP3 inflammasome activation and cell death. *Cell Mol Immunol*. 2021;18(9):2114–2127. doi:10.1038/s41423-021-00740-6
40. Liu J, Zhou J, Luan Y, et al. cGAS-STING, inflammasomes and pyroptosis: an overview of crosstalk mechanism of activation and regulation. *Cell Commun Signal*. 2024;22(1):22. doi:10.1186/s12964-023-01466-w
41. Shi J, Gao W, Shao F. Pyroptosis: gasdermin-mediated programmed necrotic cell death. *Trends Biochem Sci*. 2017;42(4):245–254. doi:10.1016/j.tibs.2016.10.004
42. Burdette BE, Esparza AN, Zhu H, Wang S. Gasdermin D in pyroptosis. *Acta Pharm Sin B*. 2021;11(9):2768–2782. doi:10.1016/j.apsb.2021.02.006